31st International Congress on Sound and Vibration

6 Sun - 11 Fri, July 2025
ICSV31
Incheon, Korea
31st International Congress on Sound and Vibration
The annual congress of the International Institute of Acoustics and Vibration (IIAV)

A HYBRID LEARNING-BASED ACTIVE NOISE CONTROL ALGORITHM FOR ENCAPSULATED STRUCTURES WITH LINEAR TIME-VARYING CHARACTERISTICS

Alkahf ABOUTIMAN
Department of Mechanical Engineering, Politecnico di Milan, Milan, 20156, Italy
email: alkahfahmat.aboutiman@polimi.it

Hamid Reza KARIMI
Department of Mechanical Engineering, Politecnico di Milan, Milan, 20156, Italy
email: hamidreza.karimi@polimi.it

Francesco RIPAMONTI
Department of Mechanical Engineering, Politecnico di Milan, Milan, 20156, Italy
email: francesco.ripamonti@polimi.it

This paper proposes a hybrid approach that integrates deep learning with ANC algorithms to enhance noise attenuation in these environments. A simulated test environment is developed using the finite element method (FEM) to model an encapsulated linear time varying (LTV) system. This model enables the extraction of frequency responses from the reference, primary, and secondary paths, revealing non-minimum phase (NMP) characteristics that further complicate noise control due to phase delays and inverted dynamics. To address these challenges, a hybrid ANC framework is proposed, integrating a two-dimensional convolutional neural network (2D CNN) with selective fixed-filter ANC (SFANC) and a normalized least mean square (NLMS) algorithm. The 2D CNN utilizes spectrogram inputs to dynamically select the most suitable pre-trained control filters for varying primary noise conditions, while the NLMS algorithm continuously updates the filter coefficients in real time to adapt to the LTV system. The results demonstrate that the proposed hybrid approach outperforms conventional SFANC methods, achieving more effective noise reduction, improved robustness, and optimized response time.
Keywords: Finite elements method, Active noise control, Encapsulated structure, Linear Time Varying system

1. Introduction

Encapsulated environments such as trains, cars, and airplanes can greatly benefit from active noise control (ANC) systems, which offer an advanced solution for mitigating unwanted noise [1], [2]. By leveraging strategically placed sensors to detect noise and actuators to generate anti-noise signals in phase opposition, these systems achieve effective noise cancellation in targeted areas. This technology enhances passenger comfort by reducing disturbances caused by both external and internal sound sources. However, implementing ANC in such dynamic environments presents several challenges, particularly in maintaining stable performance across a broad frequency spectrum. Addressing these

challenges requires advanced techniques, including precise acoustic modeling, robust path identification, and adaptive control algorithms [3], [4].

One of the fundamental obstacles to effective noise reduction lies in the dynamic nature of the control of the environment. In systems where acoustic propagation paths exhibit non-minimum phase characteristics, the initial control signal may introduce undesired effects such as transient overshoot, phase shift, or delay in the compensation. This phenomenon complicates the convergence of adaptive algorithms and imposes fundamental limitations on system performance [5], [6]. Furthermore, in environments where system properties vary over time such as encapsulated structures subjected to changing operational conditions (e.g., speed, temperature, structural load), traditional control solutions become less effective, necessitating the development of more robust and flexible approaches [7], [8].

This study introduces an ANC algorithm specifically designed for an encapsulated structure referred to as the "noise box," which replicates the acoustic environment of a vehicle cabin. The proposed algorithm, SFANC-NLMS, builds upon previous research to enhance noise reduction efficiency in complex acoustic conditions. Inspired by [9], it integrates a lightweight two-dimensional convolutional neural network (2D CNN) running on a co-processor to dynamically select the most suitable pre-trained control filter based on the encountered noise type. Concurrently, the NLMS algorithm continuously updates the filter coefficients at the sampling rate, ensuring real-time adaptability to changing acoustic conditions. This hybrid approach enables the system to maintain effective noise suppression even as system properties evolve, addressing the challenges posed by LTV systems.

2. FEM model of the encapsulated structure

2.1 The acoustic environment

In the finite element model, a specifically designed cavity, termed the "Noise Box," was utilized to emulate the acoustic environment inside a vehicle. To efficiently simulate the sound field within this enclosed structure, a strategic simplification was applied: rather than modeling both internal and external sound fields an approach that would have significantly increased computational demands only the air cavity and the vibrating portion of the plate were included in the model. The Noise Box features a pentagonal prism shape with an additional compartment housing the vibrating plate. This enclosure is sealed with a rectangular aluminum plate, measuring. The key physical properties of the plate material are summarized in Table 1.

Table 1: Physical properties of the plate material

Property	Value
Thickness, t (m)	0.0004
Density, ρ (kg/m^3)	2700 kg/m^3
Modulus of elasticity, E (Pa)	70e9 Pa
Poisson's ratio, ν	0.33

A schematic representation of the Noise Box, including its dimensional details, is presented in Figure 1 The finite element analysis was conducted using COMSOL Multiphysics R© as referenced in [10].

Table 2: Physical properties of the plate material

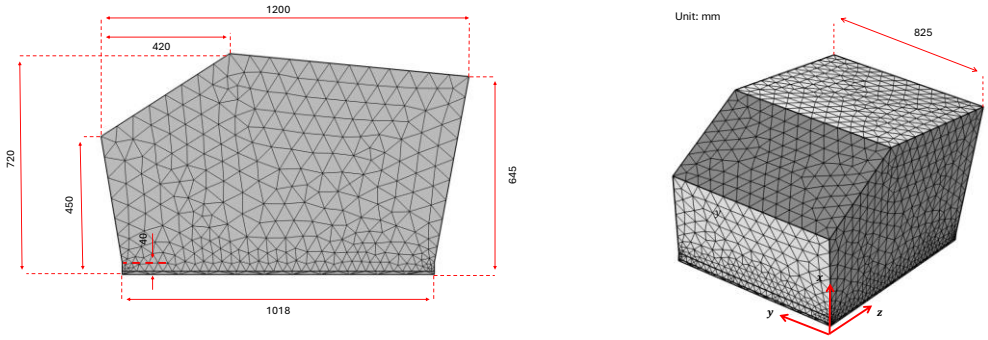

(a) (b)

Figure 1 : Geometry of the Noise Box FEM models in (a) 2D and (b) 3D.

2.2 Physics

For numerical meshing, triangular elements are utilized for the panel, maintaining a maximum element size of 0.024 m, whereas tetrahedral elements are applied to the air cavity. The upper mesh size limit λ_{max} is determined as $\lambda_{max} = c/(N \cdot f_{max})$ where $c = 343\ m/s$ represents the speed of sound in air, and $f_{max} = 1000\ Hz$ denotes the highest frequency of interest. The number of mesh elements per wavelength N is set between 7 and 10, as recommended for accurate acoustic wave propagation modeling [11]. This vibroacoustic simulation necessitates a Multiphysics framework, incorporating strong acoustic-structure coupling to account for the interaction between the aluminum panel and the enclosed air cavity.

The aluminum plate was represented in a three-dimensional model using the Shell physics module, incorporating quadratic shell elements based on the Mindlin-Reissner theory. To accurately capture both thin and thick shell responses, the Mixed Interpolation of Tensorial Components (MITC) approach was employed. Given the plate's extremely small thickness-to-span ratio h/a which is significantly below the 1/20 threshold Kirchhoff-Love theory is the most appropriate model for this study [12], [13]. The shell elements feature three degrees of freedom (DOF) corresponding to displacements in the x, y and z directions. Structural damping is incorporated using an isotropic loss factor $\eta = 0.003$, selected based on median damping values for aluminum plates [14]. The plate's edges are fully constrained within the cavity. The acoustic domain of the cavity is simulated using the "Acoustics Frequency Domain" approach. Assuming a constant atmospheric pressure of 1 atm, the air properties are defined as $\rho_0 = 1.2043\ kg/m^3$ and $c = 343.2\ m/s$ at 20°C. All external walls are modeled as acoustically rigid, ($\overline{v_n} = 0$). To approximate a reverberation chamber, impedance is set at $Z_0 = 100 \times \rho_0 \times c$.

2.3 FRF Computation

To identify these paths, the frequency response of the Noise Box is evaluated for three different propagation routes. The disturbance is represented as a plane wave, with its corresponding acoustic pressure applied to the aluminum plate. This pressure consists of the sum of the incident wave pressure p_{inc} and the reflected pressure p_{refl}, as defined in equations (1), (2).

$$p_{inc} = Ae^{i\phi}e^{i(k_x x + k_y y + k_z z)}e^{i\Phi} \quad (1)$$

$$p_{refl} = Ae^{i\Phi}e^{i(-k_x x + k_y y + k_z z)}e^{i\Phi} \tag{2}$$

Here, $k_x = k \cdot \sin(\theta) \cdot \sin(\phi), k_y = k \cdot \sin(\theta) \cdot \cos(\phi), k_z = k \cdot \cos(\theta)$ are the wave numbers, while Φ denotes the wave's phase. The angles θ and ϕ define their propagation direction. The frequency response analysis starts with a Single-Input-Single-Output (SISO) system. Sensors are represented as 'Point Probes,' each capturing distinct physical quantities: a reference accelerometer, an error microphone, and a canceling loudspeaker. The frequency response of the reference path is the ratio of the incident acoustic pressure (Pa) to the plate's normal acceleration m/s^2, yielding units of (m/s^2)/Pa. The response of the primary path is the ratio of the incident acoustic pressure to the error microphone's measured pressure (Pa), making it dimensionless. For the secondary path the canceling loudspeaker is modeled as a monopole with a unitary volume flow rate. Its unit is $Pa/m^3 \cdot s$. Accurate FRF computation is crucial for deriving the state-space model required for control implementation. The transfer function is estimated using a residue-pole representation.

$$H(s) = \sum_n \frac{\mathrm{C_n}}{s - A_n} + D \tag{3}$$

Where $s = i\omega f$, C_n are residues, A_n are poles, and D is the direct term. The coefficients are approximated to match the computed frequency response using the AAA (Adaptive Antoulas-Anderson) algorithm [15]. The state-space model is first derived in the continuous domain and then discretized using the Zero-Order Hold (ZOH) method, assuming constant input between sampling intervals. This conversion, performed at 16 kHz, enables digital control design [16]. The resulting FRFs are shown in Figure 2.

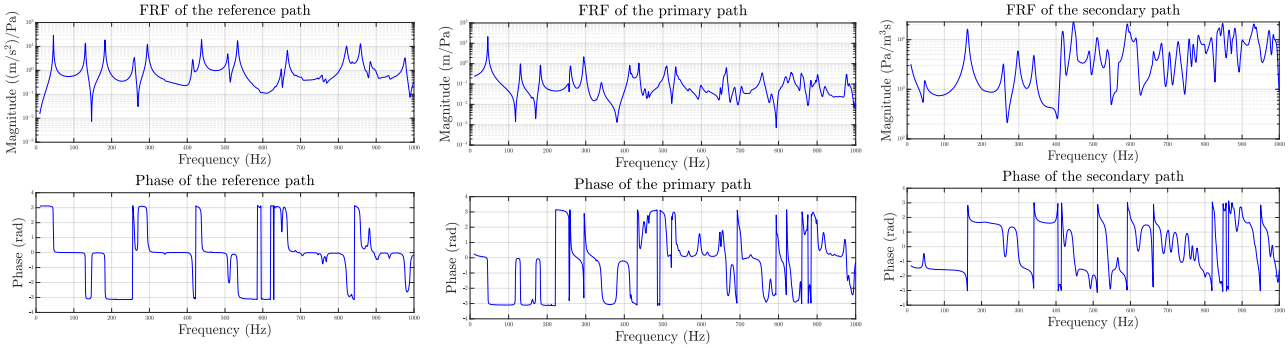

(a) (b) (c)

Figure 2: Frequency response function of the reference (a), primary (b) and secondary paths (c).

3. 2D CNN based SFANC-NLMS presentation

3.1 The SFANC-NLMS algorithm

The Selective Fixed-Filter Active Noise Control with NLMS (SFANC-NLMS) method enhances noise reduction by combining a database of pre-trained control filters with real-time adaptive filtering. It operates in two stages:

1. **Offline Pre-training**: A set of control filters is generated using the NLMS algorithm for different frequency ranges (20 Hz–1000 Hz), presented in Table 3. These filters are stored in a database for real-time selection.

Table 3: Frequency ranges for each control filter

Control filter (C_i)	Frequency range (Hz)
C_1	$20 - 1000$
C_2	$20 - 500$
C_3	$500 - 1000$

2. **Online Control**: The system analyzes the incoming noise and selects the most suitable pre-trained filter, reducing computational complexity. A convolutional neural network (CNN) assists in filter selection, while the NLMS algorithm fine-tunes the filter coefficients dynamically to adapt to real-time variations in the noise environment.

This hybrid approach ensures efficient and responsive noise cancellation, making it particularly suitable for real-time applications in dynamic acoustic environments with non-stationary characteristics. The algorithm diagram is presented in Figure 3.

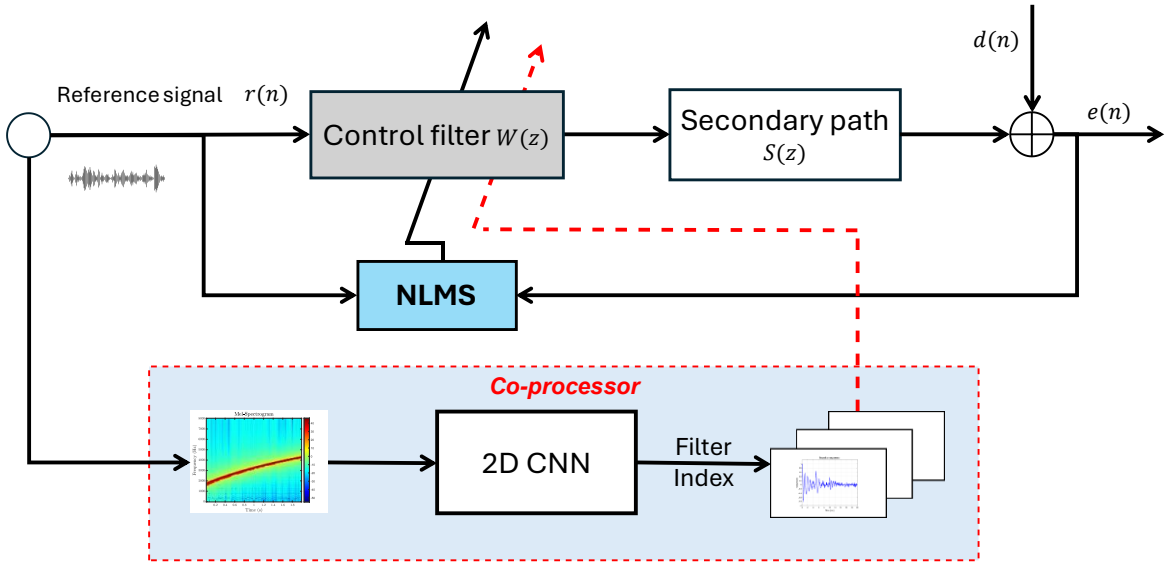

Figure 3: Block diagram of the hybrid SFANC-NLMS algorithm based on 2D CNN.

3.2 2D CNN Architecture and training

The proposed model is an optimized variant of a 2D CNN, originally inspired by [17]. Modifications were made to enhance efficiency by reducing the number of parameters, optimizing convolutional layers, and eliminating the SoftMax layer in favor of direct classification. The architecture starts with a convolutional layer to capture fundamental spectral patterns. This is followed by ReLU activation and max pooling for dimensionality reduction. The second convolutional block consists of two successive convolutional layers, increasing feature extraction to 32 maps. A max pooling operation further compresses the data before feature vectors are flattened, batch-normalized, and processed by a

fully connected layer with 15 neurons. A final dense layer produces the classification output. The full architecture is outlined in Figure 4.

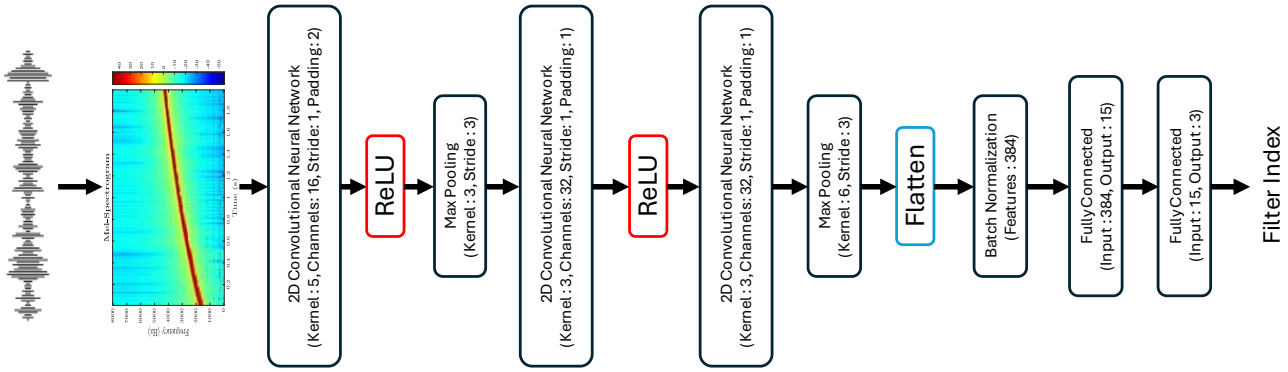

Figure 4: 2D CNN Architecture.

The network processes Mel spectrograms derived from 16 kHz audio signals. These spectrograms are computed using a 1024-point FFT, a hop size of 512, and 64 Mel filter banks, ensuring a fixed frequency resolution. The number of time frames depends on the signal duration, yielding 31 frames per second of input data.

The model was trained on a dataset consisting of 80,000 Mel spectrograms for training and 2,000 for validation and testing. These spectrograms were derived from broadband noise recordings at 16 kHz, with randomized frequency content. Each sample corresponds to a 1-second audio segment. Training was conducted using the Adam optimizer with a learning rate of 0.0001, a batch size of 250, and over 30 epochs. To mitigate overfitting, L2 regularization 0.0001 was applied to all trainable parameters.

The performance of this CNN was benchmarked against various architectures, including the 2D CNN from [17], ShuffleNet [18], MobileNet [19] and DenseNet [20]. As summarized in Table 4 , the proposed model achieves high classification accuracy while maintaining a significantly lower parameter count, optimizing both efficiency and performance.

Table 4: Test accuracy and parameter comparison for various networks.

Network	Test Accuracy	Parameters
Proposed method	99.35 %	20,959
2D CNN [17]	96.30 %	25,855
ShuffleNet [18]	98,80 %	246,110
MobileNet [19]	97,45 %	2,457,721
DenseNet [20]	99,40 %	6,954,759

4. Results of ANC under LTV conditions

In this section, simulations are performed using a single-channel ANC system. The sampling rate is set to 16 kHz, and the control filter length is fixed at 8192 taps. The state-space coefficients presented are used to model the reference, primary, and secondary paths. Additionally, three pre-trained control filters are employed. The NLMS algorithm is applied with a step size of 0.00015 to optimize the control filters for each white noise signal. To analyze robustness, a 15-second random noise filtered between 20 and 450 Hz was used, with the SNR of the primary path varying over time: it remained constant during

the first third, was reduced to 5 dB in the second third, and increased to 8 dB in the final third. The time and frequency domain results are illustrated in Figure 5.

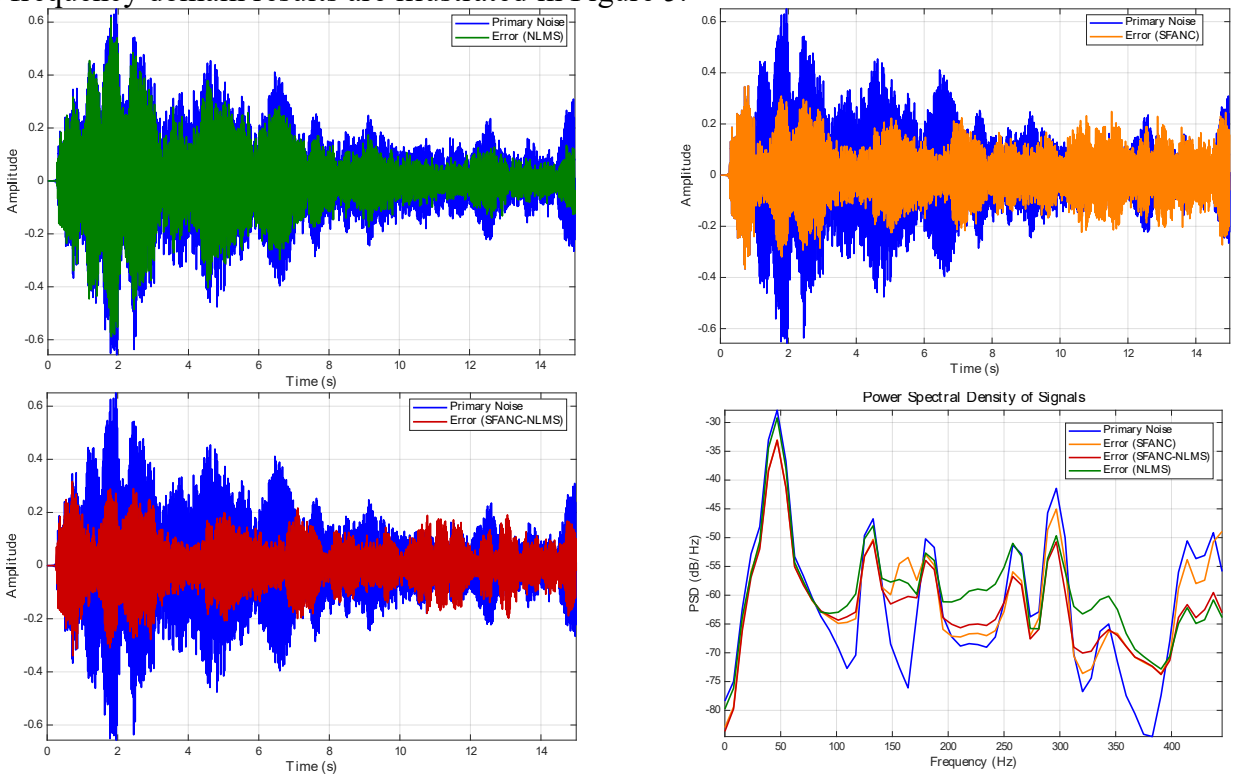

Figure 5: Graphics in time domain and PSD of the varying primary noise and error obtained using different ANC algorithms. The control is applied to broadband noise.

As a result, we can conclude that SFANC-NLMS outperforms all other algorithms under LTV conditions. In the frequency domain, a waterbed effect is observed, which is attributed to the non-minimum phase characteristics of the environment. However, thanks to its adaptive properties, SFANC-NLMS effectively adjusts to time-varying conditions. The noise reduction achieved by each algorithm is as follows: 1.5 dB for NLMS, 4.7 dB for SFANC, and 5.3 dB for SFANC-NLMS.

5. Conclusion

This study investigated the performance of an advanced active noise control (ANC) algorithm, SFANC-NLMS, designed for encapsulated environments such as vehicle interiors. By leveraging a hybrid approach that combines a lightweight 2D CNN for adaptive filter selection and an NLMS algorithm for real-time coefficient updates, SFANC-NLMS demonstrated superior noise reduction capabilities compared to conventional ANC methods.

Through simulations in a noise box environment, the proposed algorithm was evaluated under both stationary and non-stationary noise conditions, as well as time-varying primary paths. The results showed that SFANC-NLMS effectively adapts to dynamic acoustic environments, achieving a noise reduction of 5.3 dB, outperforming SFANC (4.7 dB) and NLMS (1.5 dB). Additionally, while the presence of non-minimum phase characteristics introduced a waterbed effect in the frequency domain, the adaptive nature of SFANC-NLMS allowed it to mitigate these limitations more effectively than traditional approaches.

Overall, this study highlights the potential of integrating adaptive learning-based techniques with conventional ANC strategies to enhance noise reduction in challenging acoustic environments. Future work will focus on optimizing computational efficiency for real-time embedded applications and extending the approach to multi-channel ANC systems for broader applicability in practical scenarios.

Acknowledgements

The work was supported by the project IN-NOVA: Active reduction of noise transmitted into and from enclosures through encapsulated structures, which has received funding from the European Union's Horizon Europe program under the Marie Sklodowska-Curie grant agreement no. 101073037.

REFERENCES

[1] C. Fuller, C. Hansen, and S. Snyder, "Active control of sound radiation from a vibrating rectangular panel by sound sources and vibration inputs: an experimental comparison," *Journal of Sound and Vibration*, vol. 145, no. 2, pp. 195–215, 1991.

[2] M. Misol, S. Algermissen, and H. P. Monner, "Experimental investigation of different active noise control concepts applied to a passenger car equipped with an active windshield," *Journal of Sound and Vibration*, vol. 331, no. 10, pp. 2209–2219, 2012.

[3] W. Belgacem, A. Berry, and P. Masson, "Active vibration control on a quarter-car for cancellation of road noise disturbance," *Journal of Sound and Vibration*, vol. 331, no. 14, pp. 3240–3254, 2012.

[4] A. Aboutiman, R. Shams, H. R. Karimi, F. Ripamonti, and M. Pawełczyk, "Active noise control in encapsulated structures with non-minimum phase characteristics using a Kalman filter approach," *Journal of Sound and Vibration*, vol. 615, p. 119187, 2025, doi: https://doi.org/10.1016/j.jsv.2025.119187.

[5] A. A. Milani, G. Kannan, and I. M. Panahi, "On maximum achievable noise reduction in ANC systems," in *2010 IEEE International Conference on Acoustics, Speech and Signal Processing*, IEEE, 2010, pp. 349–352.

[6] L. Wu, X. Qiu, and Y. Guo, "A generalized leaky FxLMS algorithm for tuning the waterbed effect of feedback active noise control systems," *Mechanical Systems and Signal Processing*, vol. 106, pp. 13–23, 2018.

[7] R. Castane-Selga and R. S. S. Peña, "Active noise hybrid time-varying control for motorcycle helmets," *IEEE Transactions on control systems technology*, vol. 18, no. 3, pp. 602–612, 2009.

[8] A. Aboutiman *et al.*, "Subjective perception analysis of active noise control algorithms in an encapsulated structure: An experimental study," *Applied Acoustics*, vol. 239, p. 110823, 2025.

[9] Z. Luo, D. Shi, and W.-S. Gan, "A hybrid sfanc-fxnlms algorithm for active noise control based on deep learning," *IEEE Signal Processing Letters*, vol. 29, pp. 1102–1106, 2022.

[10] L. Liu, "Design, simulation and testing of a coupled plate-cavity system targeted for vehicle interior noise analysis and control," 2021.

[11] R. Astley, G. Macaulay, and J. Coyette, "Mapped wave envelope elements for acoustical radiation and scattering," *Journal of Sound and Vibration*, vol. 170, no. 1, pp. 97–118, 1994.

[12] L. Cremer and M. Heckl, *Structure-borne sound: structural vibrations and sound radiation at audio frequencies*. Springer Science & Business Media, 2013.

[13] D. Chapelle and K.-J. Bathe, *The finite element analysis of shells-fundamentals*. Springer Science & Business Media, 2010.

[14] P. Lenk and G. Coult, "Damping of glass structures and components," presented at the Challenging Glass Conference Proceedings, 2010, pp. 341–350.

[15] Y. Nakatsukasa, O. Sète, and L. N. Trefethen, "The AAA algorithm for rational approximation," *SIAM Journal on Scientific Computing*, vol. 40, no. 3, pp. A1494–A1522, 2018.

[16] T. J. Moir and T. J. Moir, *Rudiments of Signal Processing and Systems*. Springer, 2022.

[17] D. Shi, B. Lam, K. Ooi, X. Shen, and W.-S. Gan, "Selective fixed-filter active noise control based on convolutional neural network," *Signal Processing*, vol. 190, p. 108317, 2022.

[18] Z. Luo, D. Shi, J. Ji, X. Shen, and W.-S. Gan, "Real-time implementation and explainable AI analysis of delayless CNN-based selective fixed-filter active noise control," *Mechanical Systems and Signal Processing*, vol. 214, p. 111364, 2024.
[19] S. Adapa, "Urban sound tagging using convolutional neural networks," *arXiv preprint arXiv:1909.12699*, 2019.
[20] G. Huang, Z. Liu, L. Van Der Maaten, and K. Q. Weinberger, "Densely connected convolutional networks," in *Proceedings of the IEEE conference on computer vision and pattern recognition*, 2017, pp. 4700–4708.